

## Iterative solutions to quantum-mechanical problems

C. J. Tymczak, G. S. Japaridze, C. R. Handy, and Xiao-Qian Wang

*Department of Physics and Center for Theoretical Studies of Physical Systems, 223 James P. Brawley Drive,  
Clark Atlanta University, Atlanta, Georgia 30314*

(Received 4 May 1998)

We have shown [Phys. Rev. Lett. **80**, 3673 (1998)] that the wave-function representation  $\Psi(\xi) = \sum_j a_j[E] \xi^j R_\beta(\xi)$ , developed in either configuration or momentum space for a suitable *reference function*  $R_\beta(\xi)$ , defines a highly accurate, multidimensional, energy-quantization procedure, once the convergent zeros of the power-series expansion coefficients  $a_j[E]=0$  ( $j \rightarrow \infty$ ) are determined. In this paper we amplify the underlying analysis and also examine some of the consequences for generating accurate wave functions.  
[S1050-2947(98)04210-3]

PACS number(s): 03.65.Ge, 02.30.Hq

### I. INTRODUCTION

The use of power-series expansions is one of the most basic techniques for solving differential equations, including the Sturm-Liouville problem defined by the Schrödinger wave equation [1]. Such methods, in the context of eigenvalue problems, are limited because they are essentially local, not global, approximation techniques.

However, if we combine such a philosophy with a slightly different representation for the wave function

$$\Psi(x) = A(x)R_\beta(x),$$

where  $R_\beta$  defines an appropriate *reference function*, then the power-series expansion for  $A(x)$  (assuming analyticity at  $x=0$ ) is better suited for addressing the global issues relevant to determining the eigenenergies. This is because the expansion  $A(x) = \sum_i a_i x^i$ , combined with the reference function, can be interpreted as the projection of the wave function onto the (nonorthogonal) basis  $\{x^i R_\beta(x) | 0 \leq i < \infty\}$ :

$$\Psi(x) = \sum_i a_i(E) x^i R_\beta(x). \quad (1)$$

Recently [2], we have studied the latter perspective by utilizing Hill-determinant motivated relations in order to derive energy-quantization approximations based on explicit analysis of the energy  $E$ -dependent power-series coefficients  $a_i$ . For instance, in the case of one-dimensional parity-invariant problems,  $a_i(E)$  is a polynomial in  $E$ . It was shown that the roots of the equation  $a_i(E_n^{(i)})=0$  converge to the discrete state energies, as  $i \rightarrow \infty$ :

$$a_i(E_n^{(i)})=0 \Rightarrow \lim_{i \rightarrow \infty} E_n^{(i)} = E_n^{(\text{exact})}. \quad (2)$$

This is very convenient, in comparison to explicitly working with the Hill determinant, since the  $a_i(E)$  coefficients usually satisfy a recursive structure that is readily programmable, to arbitrary order. Thus, for problems in one space dimension involving  $N$  basis states  $[x^i R_\beta(x), 0 \leq i \leq N-1]$ , our analysis of  $a_N(E)=0$  reduces the quantization problem to a one-dimensional projection subspace analysis.

This computational efficiency extends to more complex problems in multidimensions, formulated in either configuration or momentum space. In the latter case, Eq. (1) is implemented in the Fourier space, which in turn, through its inverse Fourier transform, defines another approximation for the configuration-space wave function. This is discussed below.

In this paper we present a comprehensive overview, with examples, of the entire formalism. Whereas the cited investigation by us only focused on obtaining the eigenenergies, the present work examines some of the consequences for the wave functions as well.

This paper is organized as follows. In Sec. II we present the results for various one-dimensional parity invariant systems such as the quartic anharmonic oscillator and the double-well quartic anharmonic potential. We then generalize the method to include parity-nonconserving potentials and a transcendental potential. Included is a discussion on criteria for selecting appropriate reference functions. In Sec. III we extend the formalism to momentum space. Several one-dimensional examples are (re)examined. We then proceed to extend this formalism to radial problems, which also allows us to solve potential well problems (which are not readily accessible in configuration space). In Sec. IV we examine the multidimensional implementation of our formalism. In particular, we consider the two-dimensional anharmonic oscillator potential  $V(x,y) = x^2 + y^2 + gx^2y^2$ , the quadratic Zeeman problem, and the hydrogen diatomic ion. In the Appendix we provide a theoretical justification for our quantization formula, as given in Eq. (2).

### II. CONFIGURATION-SPACE ANALYSIS

#### A. Parity-invariant potentials

We now demonstrate the capabilities of the preceding method. For completeness, we note that for the case of exactly solvable potentials, where the wave function can be expressed as a polynomial multiplied by a suitable reference function, our method reproduces the exact solutions.

Consider a nonexactly solvable problem, such as the quartic anharmonic oscillator

TABLE I. Calculated ground- and first excited-state energies for the quartic anharmonic oscillator with  $g=1$ .

$I$	$\beta$	$n$	$E_n$
10	1/2	0	1.41
		1	4.9
	1	0	1.392
		1	4.65
40	1/2	0	1.392 349
		1	4.648 84
	1	0	1.392 351 641 4
		1	4.648 812 70
160	1/2	0	1.392 351 641 530 291
		1	4.648 812 704 212
	1	0	1.392 351 641 530 291 855 657 507 876
		1	4.648 812 704 212 077 536 377 032 91
500	8	0	1.392 351 641 530 291 855 657 507 876 609 934 184 600 066 711 220 834 088 906 349 323 877 567 431 875 646 528 590 973 563 467 791 759 121 151 375 341 738 817 445 551 624 046 383 713 043 817 869 737 001 346 093 516 81
		1	1.392 351 641 530 291 85
	Ref. [6,7]		$E_0$ $E_1$

$$H = -\frac{d^2}{dx^2} + x^2 + gx^4. \tag{3}$$

Using the reference function  $R_\beta = \exp(-\beta x^2)$ , one obtains the recursion relation

$$a_i(E) = \frac{\Omega_i a_{i-2}(E) + (1 - 4\beta^2) a_{i-4}(E) + g a_{i-6}(E)}{i(i-1)}, \tag{4}$$

where  $\Omega_i = 4\beta i - 6\beta - E$ ,  $a_i = 0$  for  $i < 0$ , and  $\{a_0 = 1, a_1 = 0\}$  or  $\{a_0 = 0, a_1 = 1\}$  for the symmetric or antisymmetric states, respectively. The value of the  $\beta$  parameter is arbitrary, but it can be optimized in order to accelerate the convergence rate of the quantization analysis. This is discussed in Sec. II C.

Table I shows the calculated energies of the ground and first excited states for  $g=1$ . Our method shows systematic convergence for increasing  $I$ , exceeding some of the high-accuracy solutions published [3–5]. As a benchmark, we also include in Table I the high-accuracy result for the ground-state energy with 150 digits. The calculation was carried out on our local workstation. Figure 1 shows the dependence of the ground-state energy on the coupling parameter  $g$  for  $0 \leq g \leq 10$ . Figures 2 and 3 show the ground- and first excited-state wave functions calculated using our expansion for selected values of the coupling constant and  $N=40$ . As can be seen from Figs. 2 and 3, we obtain excellent point-wise convergence of the wave functions on the interval  $x \in [-3, 3]$ ; however, as also can be seen in the inset of Fig. 2 (for  $g=1$ ), around  $x=4.2$  the wave function deviates from the true solution. The value of  $x$ , beyond which the wave

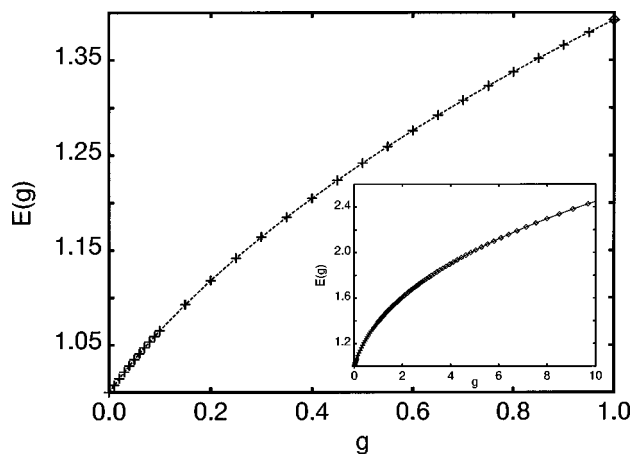


FIG. 1. Calculated ground-state energy for the quartic anharmonic oscillator for  $0 \leq g \leq 10$ .

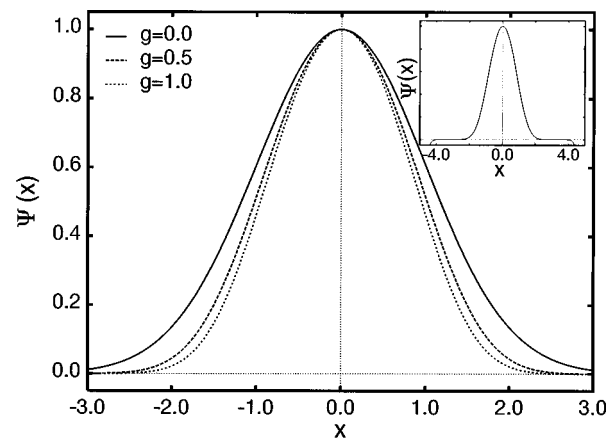


FIG. 2. Ground-state wave functions for  $g=0, \frac{1}{2},$  and 1 for the quartic anharmonic oscillator.

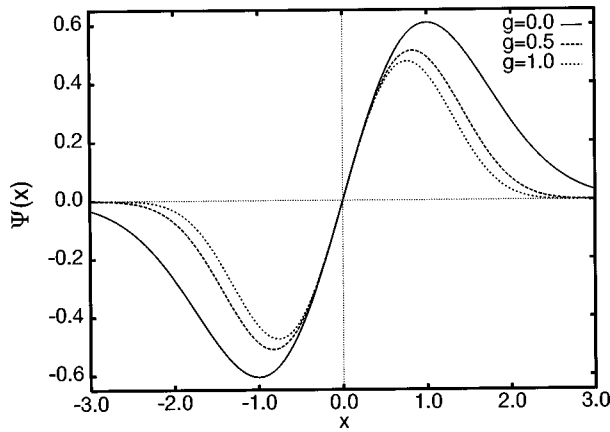


FIG. 3. First excited-state wave functions for  $g=0, \frac{1}{2},$  and 1 for the quartic anharmonic oscillator.

function starts to diverge, increases as the order of the expansion increases. As long as the desired solution admits an analytic  $A(x)$  function factor [ $\Psi(x)=A(x)R_\beta(x)$ ], our quantization procedure [Eq. (2)] should yield converging approximants to the true wave function, over an increasing domain.

The results for higher-degree potentials, such as the sextic, octic, and dectic anharmonic potentials, are given in Table II. In Fig. 4 we show the plots of the ground-state wave functions for the sextic, octic, and dectic anharmonic potentials for  $g=1$ .

An important version of the quartic anharmonic oscillator potential is the double-well problem  $V(x)=-Z^2x^2+x^4$ . It is well known that in the deep-well limit ( $Z^2 \rightarrow \infty$ ), the two lowest states are almost degenerate [6]. Application of our method (refer to Table III) readily confirms this, and by its high-accuracy nature, significantly disagrees with the predictions of de Saavedra and Buendia (SB) [6]. In particular, for  $Z^2=25$ , we observe that the quasidegenerate nature of the ground- and first excited-state energies becomes apparent only after 26 significant digits, not the 16 predicted by SB.

The generality of our method permits the study of transcendental potentials, provided the potential function  $V(x)$  admits a power-series expansion that is monotonically convergent (nonalternating). For instance, in the case of  $V(x)=\exp(x^2)-1$ , we immediately obtain the first three energy levels. Table IV shows our results for this potential.

**B. Parity-nonconserving potentials**

We can readily extend our method to include parity-nonconserving potentials. In this case, the  $a_n(E)$ 's are lin-

TABLE II. Calculated ground-state energies of the sextic, octic, and dectic anharmonic potentials for  $g=1$  calculated in configuration space ( $\beta=4, 8,$  and 12 and  $I=100, 200,$  and 300, respectively).

$V(x)$	$E_0^a$	$E_0$
$x^2+x^6$	1.435 624 619 0	1.435 624 619 003 392 315 762
$x^2+x^8$	1.491 019 895	1.491 019 895 662 204 964 166
$x^2+x^{10}$		1.546 263 512 572 345 728

<sup>a</sup>Reference [3].

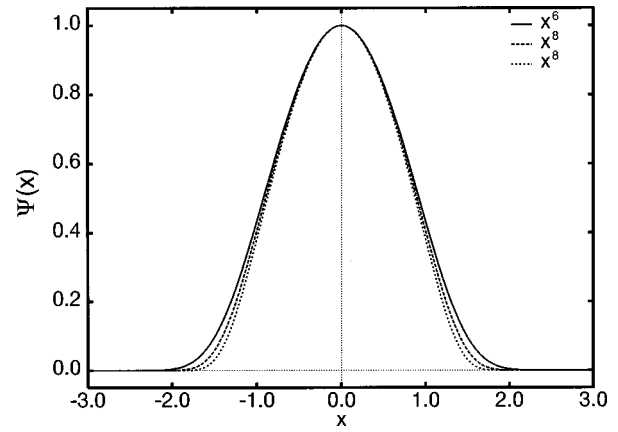


FIG. 4. Ground-state wave functions for the sextic, octic, and dectic anharmonic oscillator  $g=1$ .

early dependent on  $a_0=\Psi(0)$  and  $a_1=\Psi'(0)$  [provided  $R_\beta(0)=1$  and  $R'_\beta(0)=0$ ]. This introduces the additional complication of determining these unknowns.

Let us consider two successive  $a_n$ 's

$$a_I(E, a_0, a_1) = A_{I,0}(E)a_0 + A_{I,1}(E)a_1, \tag{5}$$

$$a_{I+1}(E, a_0, a_1) = A_{I+1,0}(E)a_0 + A_{I+1,1}(E)a_1,$$

where the  $A_{i,j}(E)$  are polynomials in  $E$  determined via iteration of the recursion equation for the  $a_n$ 's. These linear equations can be written in a more compact form

$$\vec{a}_I = \mathbf{A}^{(I)}(E)\vec{a}_0, \tag{6}$$

where

$$\vec{a}_0 = \begin{bmatrix} a_0 \\ a_1 \end{bmatrix}, \quad \vec{a}_I = \begin{bmatrix} a_I(E, a_0, a_1) \\ a_{I+1}(E, a_0, a_1) \end{bmatrix}, \tag{7}$$

$$\mathbf{A}^{(I)}(E) = \begin{bmatrix} A_{I,0}(E) & A_{I,1}(E) \\ A_{I+1,0}(E) & A_{I+1,1}(E) \end{bmatrix}.$$

TABLE III. Calculated ground- and first excited-state energies for the potential  $V(x)=-Z^2x^2+x^4$ .

$Z^2$	Parity	$E_\pm$
0	+	1.060 362 090 484 182 899 647 046 016
	-	3.799 673 029 801 394 168 783 094 188
1	+	0.657 653 005 180 715 123 059 021 723
	-	2.834 536 202 119 304 214 654 676 208
5	+	-3.410 142 761 239 829 475 297 709 653
	-	-3.250 675 362 289 235 980 228 513 775
10	+	-20.633 576 702 947 799 149 958 554 634
	-	-20.633 546 884 404 911 079 343 874 899
15	+	-50.841 387 284 381 954 366 250 996 515
	-	-50.841 387 284 187 005 154 710 149 735
25	+	-149.219 456 142 190 888 029 163 966 538
	-	-149.219 456 142 190 888 029 163 958 974

TABLE IV. First three eigenenergies for the potential  $V(x) = e^{x^2} - 1$ . [ $R_\beta(x) = e^{-\beta x^2}$  and  $\beta = 2$ .]

$I$	$n$	$E_n$
40	0	1.356 371
	1	4.633 07
	2	8.970 66
80	0	1.356 371 24
	1	4.633 078 50
	2	8.970 678 2
120	0	1.356 371 240 434
	1	4.633 078 504 735
	2	8.970 678 204 19

Applying our method to this equation requires that we set  $\vec{a}_I = \vec{0}$ . This allows us to solve for the unknown energies and initial values by taking

$$\text{Det}[\mathbf{A}^{(I)}(E)] = 0. \quad (8)$$

As  $I \rightarrow \infty$ , the roots of Eq. (8) approach the exact eigenenergies.

Let us consider two representative examples  $V(x) = gx + x^4$  and  $V(x) = gx^3 + x^4$ . Table V summarizes our results for these potentials for selected values of  $g$ . It is worth mentioning that it is possible to calculate to high precision the values of  $g$  that give  $E_0 = 0$ . For our first example we find  $g_{\text{crit}} = 1.987\,513\,084\,045\,7$  and for our second example we have  $g_{\text{crit}} = 3$ . This further underscores the utility of our

TABLE V. Ground- and first excited-state energies for the parity-nonconserving potentials  $V(x) = x^4 + gx$  and  $V(x) = x^4 + gx^3$ . ( $R_\beta = e^{-\beta x^2}$ ,  $\beta = 3$ , and  $N = 100$ .)

$V(x)$	$g$	$n$	$E_n$
$x^4 + gx$	0	0	1.060 362 090 484 182 899
		1	3.799 673 029 801 394 168
	$\frac{1}{2}$	0	1.027 526 822 910 167 805
		1	3.795 588 118 233 139 437
	1	0	0.930 546 034 189 970 049
		1	3.781 896 248 503 017 521
	$\frac{3}{2}$	0	0.773 537 208 410 451 181
		1	3.754 774 941 646 378 650
	2	0	0.562 135 610 771 295 649
		1	3.709 174 584 241 651 216
$x^4 + gx^3$	0	0	1.060 362 090 484 182 899
		1	3.799 673 029 801 394 168
	$\frac{1}{2}$	0	1.025 348 988 818 159 058
		1	3.713 901 988 923 026 496
	1	0	0.905 341 223 793 293 275
		1	3.441 398 835 169 418 870
	$\frac{3}{2}$	0	0.633 719 071 342 323 228
		1	2.938 268 791 220 008 332
	2	0	-0.025 531 976 453 041 235
		1	2.172 528 222 090 785 784

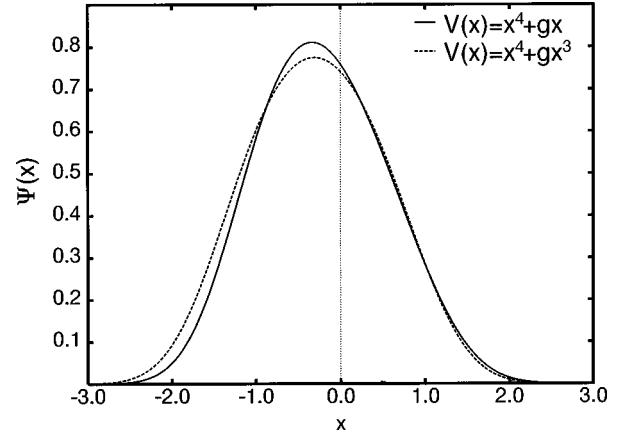


FIG. 5. Ground-state wave functions for the parity-nonconserving potentials  $x^4 + gx$  and  $x^4 + gx^3$  for  $g = 1$ .

method. Figure 5 shows the plots of both ground-state wave functions for  $g = 1$ . The lack of symmetry in the ground states is apparent.

### C. Criteria for selecting the reference function

The selection of the reference function is important. For the potential  $V(x) = x^2 + gx^6$ , our method works if  $R_\beta(x) = e^{-\beta x^n}$ ,  $n = 2$  and  $n = 3$ . For  $n = 4$ , corresponding to the asymptotic form of the wave function  $\Psi_{\text{asym}}(x) = e^{-\sqrt{g}x^{4/4}}$ , no convergent roots were observed. We have also checked this for the higher-order potentials and have found this property to be true in all cases considered.

In general,  $R_\beta(x)$  should not fall off faster than the asymptotic form of the wave function. This is because, from the perspective of the underlying Hill determinant analysis framework (refer to Appendix), the support of the basis states  $x^i R_\beta(x)$  should not be (significantly) smaller than that of the solution  $\Psi(x)$ . Such behavior complicates the extension of our method to potential wells, where the wave function falls off asymptotically as  $\Psi(r) \rightarrow e^{-\sqrt{|E|}r}$ . However, this difficulty can be circumvented by transforming our formalism into a momentum-space representation and then recovering the solution through an application of the inverse Fourier transform. This is discussed in Sec. III.

As stated earlier for the quartic anharmonic potential case, the convergence rate of our results can be significantly improved through an optimal choice of  $\beta$ . Usually, increasing  $\beta$  leads to a faster decrease in the asymptotic behavior of the reference function. Since the reference function normally decrease slower than the true wave function, increasing the value of  $\beta$  can be seen as a way to improve the correlation between the true solution and the expansion in Eq. (1), thereby speeding up the numerical convergence behavior. Evidence of this is readily apparent, particularly for increasing expansion order  $I$ ,  $a_I(E_n^{(I)}) = 0$ . Refer to Fig. 6, which shows improved (expanded) range of  $\beta$  values, with increasing expansion order, yielding accurate results.

In Fig. 7 we plot  $\log_{10}|E_0 - R_{10}(\beta)|$  and  $\log_{10}|E_0 - R_{20}(\beta)|$  vs  $\beta$ , where  $E_0$  is the ground-state energy of the quartic anharmonic oscillator. Referring to Fig. 7, as the order of the calculation increases (i) the range of  $\beta$ , leading to accuracies better than  $10^{-10}$ , increases and (ii) the  $\beta$

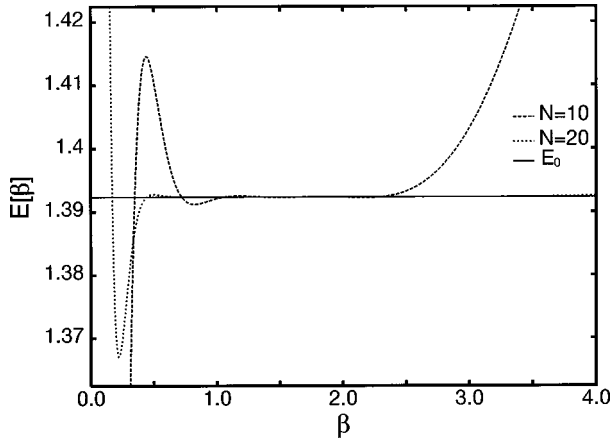


FIG. 6. First root of  $a_{10}(E, \beta)$  and  $a_{20}(E, \beta)$  vs  $\beta$  for the quartic anharmonic oscillator. The solid line is the ground-state energy.

value corresponding to optimal accuracy increases. This behavior is confirmed by other examples in this work. The determination of the optimal  $\beta$  is still not completely understood; we are in the process of developing a more complete approach, to be presented elsewhere.

### III. MOMENTUM-SPACE ANALYSIS

There are several compelling reasons for extending the preceding formalism to momentum (Fourier) space. The first of these is that by so doing, we can achieve a more global analysis of the quantization problem. That is, a power-series expansion for the momentum-space configuration  $\hat{\Psi}(k) = \mathcal{A}(k)\hat{R}_\beta(k)$  is sensitive to the small momentum (large spatial scale) structure of the physical system. Upon determining the power-series expansion representation for  $\mathcal{A}(k)$  and inverting the (truncated) expansion

$$\hat{\Psi}(k) = \left( \sum_{j=0}^{\infty} \alpha_j k^j \right) \hat{R}_\beta(k)$$

through the inverse Fourier transform, one expects to see improved global convergence for the configuration-space representation.

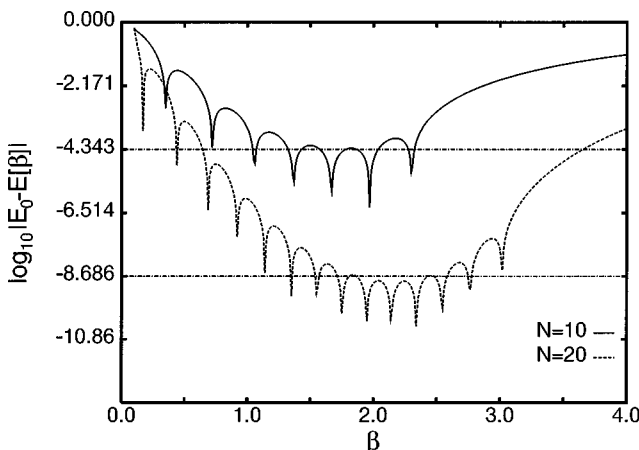


FIG. 7. Logarithm of the error of the first roots of  $a_{10}(E, \beta)$  and  $a_{20}(E, \beta)$  from the ground-state energy for the quartic anharmonic oscillator.

Of course, transforming the (second-order differential) Schrödinger operator into momentum space increases the order of the generated momentum-space differential equation. This introduces more unknown parameters into the problem, in a manner analogous to the parity-nonconserving case studied previously. Within our particular approach, these additional parameters correspond to the *missing moment* variables introduced in the eigenvalue moment method (EMM) quantization formalism developed by Handy and Bessis [7].

A second motivation for extending our formalism into momentum space is that it provides a convenient estimation theory for the EMM missing moments. It has been established that moment quantization is equivalent to continuous wavelet transform theory [8]. An important component of such an analysis is the determination of the energy and corresponding missing moment values. This is readily obtainable through the methods presented here.

Consider  $\Psi(x)$  to be symmetric, for simplicity. Its Fourier transform is generally analytic with a power-series expansion of the form

$$\hat{\Psi}(k) = \frac{1}{\sqrt{2\pi}} \int_{-\infty}^{\infty} dk e^{-ikx} \Psi(x) = \frac{1}{\sqrt{2\pi}} \sum_{\rho=0}^{\infty} \frac{(-k^2)^\rho}{(2\rho)!} u(\rho), \quad (9)$$

involving the moments

$$u(\rho) = \int_{-\infty}^{\infty} x^{2\rho} \Psi(x) dx. \quad (10)$$

For any rational fraction (multidimensional) potential, the moments will satisfy a finite-difference moment equation of effective order  $m_s + 1$ , which is problem dependent. This means that all of the moments depend linearly on the first  $m_s + 1$  (missing) moments. We can represent this through the relations

$$u(\rho) = \sum_{\ell=0}^{m_s} M_{\rho, \ell}(E) u(\ell), \quad (11)$$

where the  $M_{\rho, \ell}(E)$ 's are known and satisfy the initialization conditions  $M_{\rho, \ell}(E) = \delta_{\rho, \ell}$  for  $0 \leq \rho, \ell \leq m_s$ .

Taking  $\hat{R}_\beta(k) \equiv e^{-\beta k^2}$ , for convenience, one can determine  $\mathcal{A}(k)$  by expanding  $e^{\beta k^2} \sum_{\rho=0}^{\infty} [(-k^2)^\rho / (2\rho)!] u(\rho)$ . This leads to the representation

$$\hat{\Psi}(k) = \frac{1}{\sqrt{2\pi}} \left( \sum_{n=0}^{\infty} \alpha_n [E, u(0), \dots, u(m_s)] (-k^2)^n \right) e^{-\beta k^2}, \quad (12)$$

where

$$\alpha_n [E, u(0), \dots, u(m_s)] = \sum_{\ell=0}^{m_s} D_{n, \ell}(E) u(\ell) \quad (13)$$

and

$$D_{n, \ell}(E) = \sum_{j=0}^n \frac{(-\beta)^j M_{n-j, \ell}(E)}{j! [2(n-j)]!}. \quad (14)$$

TABLE VI. Calculated ground-state energies of the quartic, sextic, and octic anharmonic potentials for  $g=1$  calculated in momentum space. The first three entries correspond to the  $m_s=1,2,3$  missing moment problems, respectively. The last entry corresponds to the  $m_s=0$  missing moment reformulation for the sextic anharmonic oscillator.

$V(x)$	$E_0^a$	$E_0$
$x^2+x^4$	1.392 351 641 530	1.392 351 641 530 291 855 6
$x^2+x^6$	1.435 624 619 0	1.435 624 619 003 393
$x^2+x^8$	1.491 019 895	1.491 019 895 66
$x^2+x^6$	1.435 624 619 003 392 315 761 272 220	1.435 624 619 003 392 315 761 272 220

<sup>a</sup>Reference [3].

According to our quantization procedure, as detailed in the Appendix, there exists a sequence of energy and missing moment values satisfying

$$\alpha_n[E^{(n)}, \{u^{(n)}(\ell)\}] = 0,$$

converging to the physical values as  $n \rightarrow \infty$ . Since the matrix  $D_{n,\ell}(E)$  is not degenerate for all  $E$ 's, we can approximate the converging energy and missing moment sequences by considering the  $[m_s+1] \times [m_s+1]$  matrix equation

$$\sum_{\ell_2=0}^{m_s} D_{N+\ell_1, \ell_2}[E] u(\ell_2) = 0, \quad (15)$$

$0 \leq \ell_1 \leq m_s$ , and the ensuing determinant equation

$$\text{Det}(\mathbf{D}^{(N)}[E]) = 0. \quad (16)$$

After solving for the approximate eigenenergies through Eq. (16), one generates the missing moment values through Eq. (15) by imposing some convenient ( $L^1$ ) normalization, such as  $u(0) \equiv 1$ . This is also done for the multidimensional case discussed below.

Implementing the above for the quartic ( $m_s=1$ ), sextic ( $m_s=2$ ), and octic ( $m_s=3$ ) anharmonic oscillators yields the results in Table VI, which are consistent with those cited in Tables I and II. We are also able to reconstruct the wave functions in configuration space through the approximation derived from performing the inverse Fourier transform

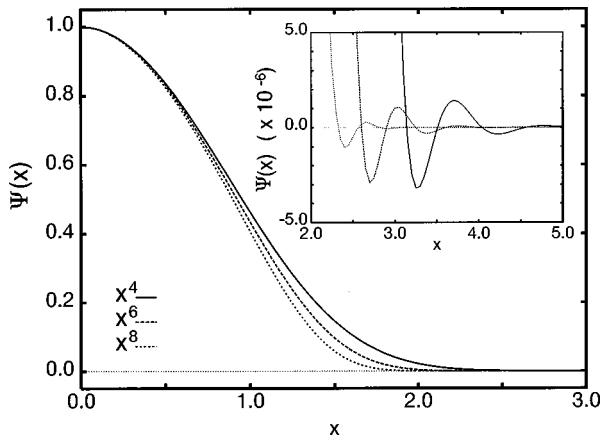


FIG. 8. Wave functions for the quartic, sextic, and octic anharmonic oscillator ( $g=1$ ), reconstructed through the momentum formulation.

$$\Psi(x) \approx \frac{1}{2\sqrt{\pi\beta}} \sum_{n=0}^N \alpha_n \frac{\partial^{2n}}{\partial x^{2n}} (e^{-x^2/4\beta}). \quad (17)$$

Figure 8 shows the reconstructed wave functions. As can be seen, the reconstructed wave function converges in a multi-scale manner (with improving small-scale behavior with increasing order). From the inset it is clear that there are small oscillations locally, which diminish as well, with increasing order  $N$  of the calculation. This behavior should be contrasted with that displayed corresponding to the application of our formalism directly in configuration space (Sec. II). There the convergence is more local in nature (i.e., essentially pointwise), with the domain of convergence increasing with the expansion order.

For completeness, we note that representations of the type in Eq. (12) were also developed in the context of a variational, Rayleigh-Ritz, missing moment formulation. Refer to Ref. [9].

### A. Zero missing moments

Some problems involve no missing moments. One of these is the aforementioned sextic anharmonic oscillator, provided one first expresses the configuration-space wave function  $\Psi(x)$  as [7(a)]

$$\Psi(x) = \Phi(x) \exp\left(\frac{\sqrt{g}}{4} x^4\right). \quad (18)$$

One then implements the momentum-space formalism on the resulting equation for  $\Phi$ , which transforms the original  $m_s=2$  problem into an  $m_s=0$  problem. The ensuing calculation yields excellent results, which we also show in Table VI. We have also calculated the ground-state energy for the potential [10]

$$V(x) = x^2 + \frac{\lambda x^2}{1 + g x^2}, \quad (19)$$

provided we represent the wave function  $\Psi(x)$  as

$$\Psi(x) = (1 + g x^2) \Phi(x) \exp\left(\frac{1}{2} x^2\right). \quad (20)$$

Table VII summarizes our results for this case, which surpass the exceptional accuracy calculated by Hodgson through an analytic continuation quantization procedure [11].

TABLE VII. First four symmetric state energies for the rational fraction potential  $V(x)=x^2 + \lambda x^2/(1+gx^2)$ .

$\lambda = g$	$n$	$E_n$
0.1	0	1.043 173 713 044 445 233 778 700 870 546 094
	2	5.181 094 785 884 700 927 110 409 072 888 3
	4	9.272 816 970 035 252 254 582 438 478 9
	6	13.339 390 726 973 551 232 933 170 5
1.0	0	1.232 350 723 406 062
	2	5.589 778 933 739
	4	9.684 042 015 236
	6	13.733 241 012 127

### B. Radial potential problems

For physical problems restricted to the non-negative real axis  $r \geq 0$  and of asymptotic form  $\Psi(r) \rightarrow e^{-\sqrt{|E|r}}$ , one cannot immediately apply the previous formalism. This is because the Fourier transform [of the extended problem satisfying  $\Psi(r)=0$  for  $r < 0$ ] will not be entire, a preferable characteristic. In addition, the asymptotic behavior as  $k \rightarrow \infty$  does not decrease sufficiently fast to justify a Gaussian-type expansion, as represented by Eq. (12).

Instead, if we map the problem onto the space defined by  $r = z^2$  for  $z \in (-\infty, \infty)$ ,  $\tilde{\Psi}(z) \equiv |z|\Psi(z^2)$ , we can proceed to apply the previous momentum-space formalism to the symmetric configuration  $\tilde{\Psi}(z)$ . Relative to this configuration, the asymptotic form  $e^{-\sqrt{|E|z^2}}$  admits an entire  $z$ -space Fourier transform. The required even-order moments

$$u(\rho) = \int_{-\infty}^{\infty} dz z^{2\rho} \tilde{\Psi}(z)$$

become

$$u(\rho) = \int_0^{\infty} dr r^\rho \Psi(r) \quad (21)$$

and satisfy a linear moment equation leading to an expression of the form in Eq. (11) [7(a)]. This permits an analysis similar to that represented by Eqs. (10)–(14). Application to the Coulomb potential yields rapidly converging estimates to the exact energies. Furthermore, reconstruction of the wave function through expansions of the type in Eq. (17),

$$\tilde{\Psi}(z) \approx \frac{1}{2\sqrt{\pi\beta}} \sum_{n=0}^N \alpha_n \frac{\partial^{2n}}{\partial z^{2n}} (e^{-z^2/4\beta}) \quad (22)$$

or

$$\Psi(r) \approx \frac{1}{2\sqrt{\pi\beta r}} \left( \sum_{n=0}^N \alpha_n \mathcal{P}_n(r) \right) e^{-r/4\beta} \quad (23)$$

[ $\mathcal{P}_n(r)$  a polynomial in  $r$ ], yield very good results, despite the singular appearance of the  $1/\sqrt{r}$  factor in Eq. (23).

In Fig. 9 we compare the true solution ( $\frac{1}{4}re^{-r/2}$ , the solid line) with the above expansion ( $N=30$ , corresponding to the open circles) and with the above expansion modulo  $\mathcal{Z}_N \equiv \sum_{n=0}^N \alpha_n \mathcal{P}_n(0)$  (since we anticipate  $\mathcal{Z}_{N \rightarrow \infty} \rightarrow 0$ ). The first ap-

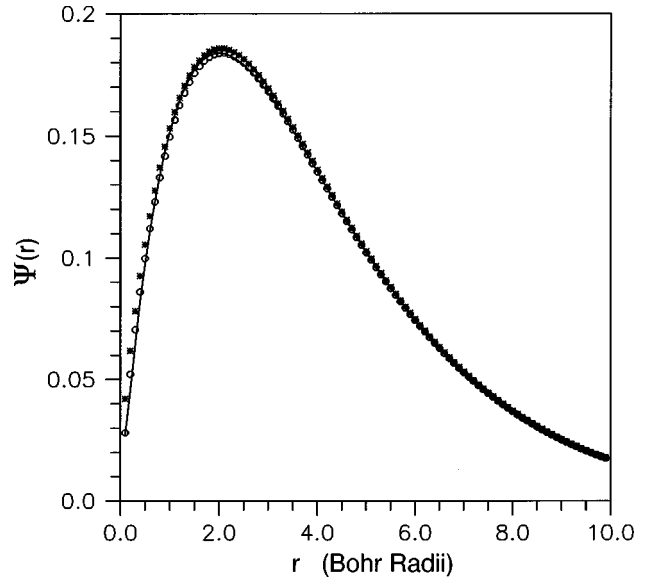


FIG. 9. Approximations to the Bohr atom ground-state solution  $\frac{1}{4}re^{-r/2}$  from the expansion in Eq. (23) (open circles) and the same expansion modulo zeroth-order sum  $\mathcal{Z}_N$  (crosses).

proximation, which includes the singularity, is actually more accurate, particularly near the origin.

All of these calculations were done for  $\beta=1$ . This is significant with respect to our earlier discussion on selecting the reference function. In particular, the asymptotic behavior of the transformed expression  $\tilde{\Psi}(z)$  goes as  $e^{-z^2/4\Gamma}$ , where  $\Gamma = \frac{1}{2}$ . Its Fourier transform will behave asymptotically as  $e^{-\Gamma k^2}$ . The choice of a Gaussian, momentum-space reference function  $e^{-\beta k^2}$  should lead to converging results for  $\beta < \Gamma = \frac{1}{2}$ . Instead, we find converging results for  $O(0.1) < \beta < O(2)$ , for  $N=30$ . In particular, good results are obtained precisely at the correct asymptotic value  $\beta = \frac{1}{2}$ . A similar analysis can be implemented with respect to the potential

$$V(r) = \frac{l(l+1)}{r^2} - \frac{1}{r+b} \quad (24)$$

(utilizing the  $m_s=2$  missing moment equations in Ref. [12]), yielding the results presented in Table VIII.

### C. One-dimensional wells

We can also study potentials of the form

$$V(x) = \frac{-f}{1+\sigma x^q} \quad (25)$$

TABLE VIII. Ground-state energy of the potential  $V(r)=l(l+1)/r^2 - Ze^2/(r+b)$ , where  $Z=1$  and  $e^2=2$ .

$l$	$b$	$E_0$
0	0.0	-1.000 000 000 00
	0.5	-1.719 643 08
	1.0	-1.000 000 000 00
1	0.0	-0.250 000 000 00
	0.5	-0.195 311 233 07
	1.0	-0.165 724 840 88

TABLE IX. First three symmetric state energies of the potential  $V(x) = -f/(1 + \sigma x^2)$ .

$f$	$\sigma$	$E_0$	$E_2$	$E_4$
1	0.0001	-0.990 074 442	-0.950 966 595	-0.913 036 071
	0.001	-0.969 109 931	-0.851 372 541	-0.744 906 128
	0.01	-0.906 983 436	-0.589 356 621	-0.367 693 169
	0.1	-0.744 761 201		
10	0.0001	-9.968 452 050	-9.842 858 475	-9.473 335
	0.001	-9.900 744 425	-9.509 665 958	-9.130 360 71
	0.01	-9.691 099 314	-8.513 725 416	-7.449 061 286
	0.1	-9.069 834 361	-5.893 566 217	-3.676 931 698

as long as we use the preceding transformation. Table IX gives the results for several different parameters ( $q = 2$ ).

#### IV. EXTENSION TO HIGHER DIMENSIONS

We outline the extension of the formalism to multidimensions through three two-dimensional problems. The two-dimensional (analytic) Fourier transform

$$\hat{\Psi}(k_1, k_2) = \frac{1}{2\pi} \int \int dx dy e^{-i(k_1 x + k_2 y)} \Psi(x, y)$$

can be expanded into the form

$$\hat{\Psi}(k_1, k_2) = \frac{1}{2\pi} \sum_{p, q} \frac{(-ik_1)^p (-ik_2)^q}{p! q!} \mu(p, q), \quad (26)$$

where the two-dimensional (Hamburger) moments are defined by

$$\mu(p, q) = \int_{-\infty}^{\infty} \int_{-\infty}^{\infty} dx dy x^p y^q \Psi(x, y). \quad (27)$$

As for the one-dimensional problems considered, the two-dimensional (Hamburger) moments also satisfy a (problem-dependent) linear, finite-difference equation of infinite order. An infinite subset of the moments (the missing moments)  $\{\mu(i_\ell, j_\ell) | 0 \leq \ell < \infty\}$  are required as initialization variables before all of the remaining moments can be determined. Thus, as in Eq. (11), all of the moments depend on these missing moments. Fortunately, any given moment depends only on a finite number of the missing moments

$$\mu(p, q) = \sum_{\ell \leq L(p, q)} M_E(p, q, \ell) \mu(i_\ell, j_\ell).$$

Now consider the representation,  $\hat{\Psi} \equiv \mathcal{A} \hat{R}$ ,

$$\hat{\Psi}(k_1, k_2) = \frac{1}{2\pi} \left( \sum_{n_1, n_2} \alpha_{n_1, n_2} (-ik_1)^{n_1} (-ik_2)^{n_2} \right) \hat{R}_\beta(k_1, k_2) \quad (28)$$

for some suitable reference function. The power-series coefficients  $\alpha_{n_1, n_2}$  depend not only on the energy parameter variable  $E$ , but also on the missing moments  $\alpha_{n_1, n_2}[E, \{\mu(i_\ell, j_\ell)\}]$ . As such, one can imitate the one-

dimensional analysis previously presented and proceed to generate the converging energy roots and corresponding missing moment values.

An important aspect of the extension of our formalism to the multidimensional case is that careful consideration must be given to determining which of the  $\alpha_{n_1, n_2}[E, \{\mu(i_\ell, j_\ell)\}]$  coefficients are to be set to zero in order to define the multidimensional counterpart to Eq. (15). An improper selection of such coefficients will not produce a converging sequence of approximants to the physical energy and corresponding missing moments.

Once the energy and missing moments have been generated, one can approximate the configuration-space solution by performing an inverse Fourier transform on Eq. (28),

$$\Psi(x) = \frac{1}{2\pi} \sum_{n_1, n_2} \alpha_{n_1, n_2} (-\partial_x)^{n_1} (-\partial_y)^{n_2} R_\beta(x, y), \quad (29)$$

where

$$R_\beta(x, y) = \frac{1}{2\pi} \int \int dk_1 dk_2 e^{i(xk_1 + yk_2)} \hat{R}(k_1, k_2).$$

One can also implement a similar procedure directly in configuration space. This involves the representation

$$\Psi(x, y) = \left( \sum_{i, j} a_{i, j} x^i y^j \right) R_\beta(x, y), \quad (30)$$

where the  $\{a_{i, j}\}$  coefficients depend, linearly, on a smaller subset, such as  $\{a_{i, 0}\}$ . Quantization can be achieved by setting a finite subset of the  $\{a_{i, j}\}$ 's to zero, for instance,  $\{a_{N, N-i} | 0 \leq i \leq N, N < \infty\}$ .

#### A. $H_{xy}$ problem

To demonstrate the effectiveness of either method, first consider the important problem defined by the Hamiltonian [13]

$$H_{xy} = -\frac{\partial^2}{\partial x^2} - \frac{\partial^2}{\partial y^2} + x^2 + y^2 + g x^2 y^2. \quad (31)$$

Limiting the analysis to the symmetric states (with respects to transformations  $x \leftrightarrow -x$ ,  $y \leftrightarrow -y$ , and  $x \leftrightarrow y$ ), the effective two-dimensional Stieltjes moments

$$u(p, q) \equiv \mu(2p, 2q) \quad (32)$$



TABLE X. First two symmetric energy levels for  $H_{xy}$  and (binding energy)  $H_{QZ}$ .

$H$	$E_{\text{ground}}$	$E_{\text{first excited}}$
$H_{xy}$ configuration space	2.195 918 085 200	7.031 272 46
$H_{xy}$ Fourier space	2.195 918 086	7.031 272 466
$H_{QZ}(B=0.1, L=22)$	0.547 526 46	0.148 089 156
$H_{QZ}(B=1, L=26)$	0.831 167 94	0.160 469 049
$H_{QZ}(B=2, L=28)$	1.022 214 0	0.173 939 7

satisfy the moment equation

$$-2p(2p-1)u(p-1,q) - 2q(2q-1)u(p,q-1) + u(p+1,q) + u(p,q+1) + gu(p+1,q+1) = Eu(p,q) \quad (33)$$

for  $p, q \geq 0$ . Because of the  $x \leftrightarrow y$  symmetry,  $u(p, q) = u(q, p)$ ; accordingly, specification of the missing moments  $\{u(i, 0) | 0 \leq i \leq N\}$  is sufficient to generate all the moments  $\{u(p, q) | 0 \leq p, q \leq N\}$  for a given value of energy parameter value  $E$ . We may represent the linear dependence on the missing moments as

$$u(p, q) = \sum_{\ell=0}^N M_E(p, q, \ell) u(\ell, 0) \quad \text{for } p, q \leq N. \quad (34)$$

The desired expansion for a Gaussian reference function is  $[\hat{\Psi}(\vec{k}) = \mathcal{A}(\vec{k}) e^{-\beta k^2}]$

$$e^{-\beta(-[k_1^2+k_2^2])} \sum_{p,q} (-k_1^2)^p (-k_2^2)^q \frac{u(p,q)}{(2p)!(2q)!} = \sum_{n_1, n_2} (-k_1^2)^{n_1} (-k_2^2)^{n_2} \alpha_{n_1, n_2} \quad (35)$$

or

$$\alpha_{n_1, n_2} = \sum_{i+p=n_1} \sum_{j+q=n_2} \frac{(-\beta)^{i+j}}{i!j!} \frac{u(p,q)}{(2p)!(2q)!}. \quad (36)$$

Incorporating the missing moment dependence from Eq. (34), we have

$$\alpha_{n_1, n_2} [E, \{u(\ell, 0)\}] = \sum_{\ell=0}^N u(\ell, 0) \sum_{i+p=n_1} \sum_{j+q=n_2} \frac{(-\beta)^{i+j}}{i!j!} \frac{M_E(p, q, \ell)}{(2p)!(2q)!}. \quad (37)$$

The configuration-space reconstruction becomes

$$\Psi(x, y) = \frac{1}{4\pi\beta} \sum_{n_1, n_2} \alpha_{n_1, n_2} \partial_x^{2n_1} \partial_y^{2n_2} e^{-(x^2+y^2)/4\beta}. \quad (38)$$

The momentum-space formalism was applied to  $\{\alpha_{n_1, n_2} | n_1 = N, 0 \leq n_2 \leq N\}$  (i.e., the coefficients set to zero). The calculated ground-state energy (Table X) agrees with that of Vrscay and Handy ( $\beta = 0.5, N = 20$ ) [13].

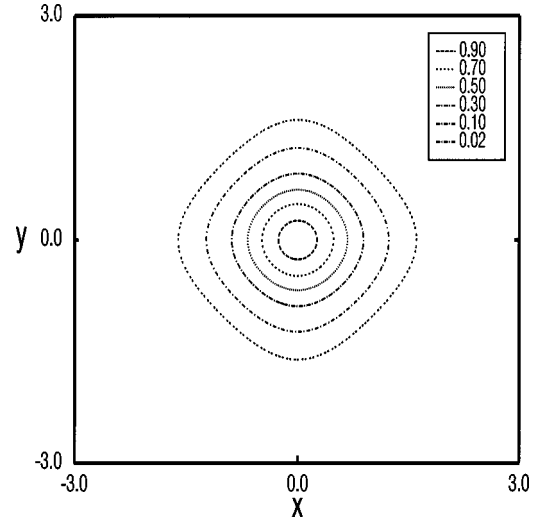


FIG. 10. Contour plot of the ground-state wave function for the two-dimensional anharmonic oscillator for  $g=1$ .

We also applied our configuration-space formalism to this problem, which depends on the set of ‘‘missing’’ coefficients  $\{\alpha_{N, N-i}[E]\}$ . Table X gives the results of our calculations in both momentum and configuration space and Figs. 10 and 11 give plots of the first two symmetric states.

### B. Quadratic Zeeman problem

Our second example, the quadratic Zeeman problem, is more conveniently solved in terms of the momentum formulation. For the  $L_z = 0$  angular momentum states of the quadratic Zeeman problem the Hamiltonian is

$$H_{QZ} = -\frac{1}{2} \nabla^2 - \frac{Z}{r} + \frac{1}{8} B^2 (x^2 + y^2). \quad (39)$$

The binding energy  $\epsilon$  is related to the total energy by  $\epsilon = B/2 - E(Z=1, B)$ . Transforming the Hamiltonian into parabolic coordinates ( $\xi = r - z > 0$  and  $\eta = r + z > 0$ ) and defining the Stieltjes moments

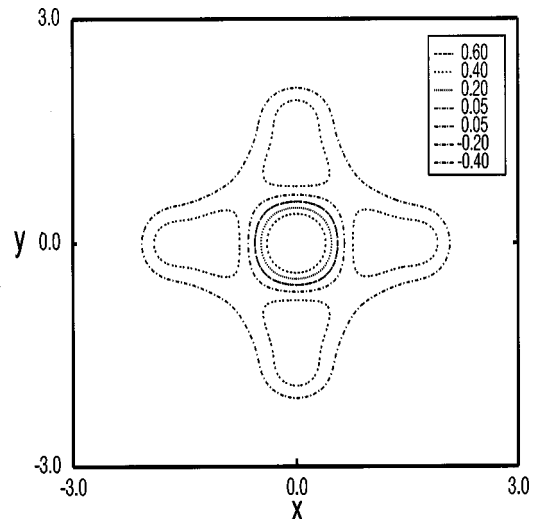


FIG. 11. Contour plot of the first symmetric excited-state wave function for the two-dimensional anharmonic oscillator for  $g=1$ .

$$u(n,m) = \int_0^\infty \int_0^\infty d\xi d\eta \xi^n \eta^m \rho(\xi, \eta)$$

for the  $\rho$  configuration satisfying [7b]

$$\Psi(\xi, \eta) = \rho(\xi, \eta) \exp\left(\frac{B}{4} \xi \eta\right)$$

allows us to generate the moment equation

$$\begin{aligned} n^2 u(n-1, m) + m^2 u(n, m-1) - \frac{1}{2} [Bn + \epsilon] u(n, m+1) \\ - \frac{1}{2} [Bm + \epsilon] u(n+1, m) + Zu(n, m) = 0. \end{aligned} \quad (40)$$

For states with the same symmetry as the ground state ( $\eta \leftrightarrow \xi$ ), the missing moments correspond to the set  $\{u(i, i) | 0 \leq i \leq L\}$ , which generate all the moments within the antidiagonals  $n+m \leq 2L+1$ ,

$$u(n, m) = \sum_{\ell=0}^{(n+m)/2} M_E(n, m, \ell) u(\ell, \ell). \quad (41)$$

As for one-dimensional radial potential problems, we are implicitly working with the extended, symmetric, configuration

$$\tilde{\rho}(\chi, \zeta) \equiv |\chi| |\zeta| \rho(\chi^2, \zeta^2),$$

where  $\xi \equiv \chi^2$  and  $\eta \equiv \zeta^2$ . It then follows that the two-dimensional Fourier transform for  $\tilde{\rho}$  exists and is analytic and the (nonzero) even-order Hamburger moments are equivalent to the Stieltjes moments  $u(n, m)$ :

$$u(n, m) = \int_{-\infty}^{\infty} \int_{-\infty}^{\infty} d\chi d\zeta \chi^{2n} \zeta^{2m} \tilde{\rho}(\chi, \zeta).$$

Reconstruction of the configuration-space solution within the  $\chi \times \zeta$  representation is then given by implementing an inverse Fourier transform on

$$\hat{\tilde{\rho}}(k_1, k_2) = \mathcal{A}(k_1, k_2) e^{-\beta(k_1^2 + k_2^2)}.$$

The formalism is identical to that of the previous problem [Eqs. (35)–(38)]. We obtain for the configuration-space wave function

$$\tilde{\rho}(\chi, \zeta) = \frac{1}{4\pi\beta} \sum_{n_1, n_2} \alpha_{n_1, n_2} \partial_\chi^{2n_1} \partial_\zeta^{2n_2} e^{-(\chi^2 + \zeta^2)/4\beta} \quad (42)$$

or

$$\begin{aligned} \rho(\xi, \eta) = \frac{1}{4\pi\beta\sqrt{\xi\eta}} \sum_{n_1, n_2} a_{n_1, n_2} (2\sqrt{\xi}\partial_\xi)^{2n_1} (2\sqrt{\eta}\partial_\eta)^{2n_2} \\ \times e^{-(\xi+\eta)/4\beta}, \end{aligned} \quad (43)$$

where  $r = (\xi + \eta)/2$  and  $r_\perp^2 = \xi \eta$ .

This expansion is consistent with our general rules for selecting appropriate reference functions since the asymptotic form of the wave functions corresponds to

$$\Psi(r_\perp, z) \rightarrow \exp\left(-\frac{1}{4}Br_\perp^2 - (2\epsilon)^{1/2}|z|\right).$$

This is valid only for  $B \neq 0$ . At  $B=0$ , the  $|z|$  becomes  $r$ . Accordingly,  $\rho(r_\perp, z) \rightarrow \exp\left(-\frac{1}{2}Br_\perp^2 - (2\epsilon)^{1/2}|z|\right)$ , which falls off faster than the  $e^{-r/2\beta}$  reference function in Eq. (43), except for purely longitudinal directions (i.e., parallel to the  $z$  axis). In such cases, the  $e^{-(2\epsilon)^{1/2}|z|}$  factor will also fall off faster than  $e^{-r/2\beta}$  if  $1/2\beta < (2\epsilon)^{1/2}$ , which is the case for all examples considered here ( $\beta=1$ ).

Excellent results are obtained if we set to zero the coefficients  $\{\alpha_{n,m} | n+m=2L+1, m \leq L\}$ , which depend on the missing moments  $\{u(i, i) | 0 \leq i \leq L\}$ . That is, by setting to zero the first set, we determine both the energy and the corresponding missing moment values in a manner identical to that in Eq. (15). Knowledge of the first  $L+1$  missing moments determines all moments within the  $2L+1$  antidiagonal  $\{u(p, q) | p+q \leq 2L+1\}$ . Accordingly, only the corresponding coefficients  $\{\alpha_{n,m} | n+m \leq 2L+1\}$  can be determined through Eq. (36) and utilized in Eqs. (42) and (43).

The first two binding energy levels (with same symmetry as ground state), for various magnetic-field values  $B \leq 2$  (a.u.), are given in Table X. In each case, we quote the number of missing moments used  $L$  ( $\beta=1$  in each case). Given  $L$ , the expansion order  $\mathcal{N}$  [the range of  $n_1$  and  $n_2$  values used in Eq. (43),  $n_1+n_2 \leq \mathcal{N}$ ] is determined by  $\mathcal{N} \leq 2L+1$ . Our results are consistent with those of Rosner *et al.* [14].

Our reconstruction analysis is only suitable for  $\rho(r_\perp, z)$  and not for the wave function itself  $\Psi(r_\perp, z)$ . This is because the expansion in Eq. (43) cannot capture the global quadratic dropoff of the true solution, at relatively low expansion orders, as described above. That is, if we use Eq. (43), together with  $\Psi = \rho e^{(B/4)r_\perp^2}$ , then the overall product will not decrease sufficiently fast, particularly for  $B \approx 2$ . The expansion in Eq. (43) is therefore only appropriate for studying the local features of the  $\rho$  solution, near the origin. Furthermore, in light of the  $1/r_\perp$  singularity in the reconstruction formula (43), which is similar to that for the Bohr case discussed earlier, one also expects that our expansion will be valid close to (but not on) the  $z$  axis as well.

Preliminary results for  $B \leq 2$  suggest that implementation of the preceding reconstruction procedure gives results in general agreement with those of Rosner *et al.* [14] and Liu and Starace [15]. In particular, upon comparing Figs. 12 and 13 [generated at  $L=O(20)$  and  $\mathcal{N}=8$ ], we see that for smaller magnetic fields, the contour plots for the ground-state configuration  $\rho(r_\perp, z)$  become broader ( $B=0.1$ ), and not as rapidly (steeply) varying as for the higher magnetic field ( $B=2$ ) case. Our results also emphasize that there is a ‘‘pinching’’ of the wave-function contours at  $z=0$ . This is intuitively obvious since both the attractive Coulombic and quadratic potentials are their strongest at  $z=0$ . This is not quite as evident from the results of Rosner *et al.* and Liu and Starace, although there is the suggestion of this in one of Liu-Starace plots [see Fig. 4(a) in Ref. [15]].

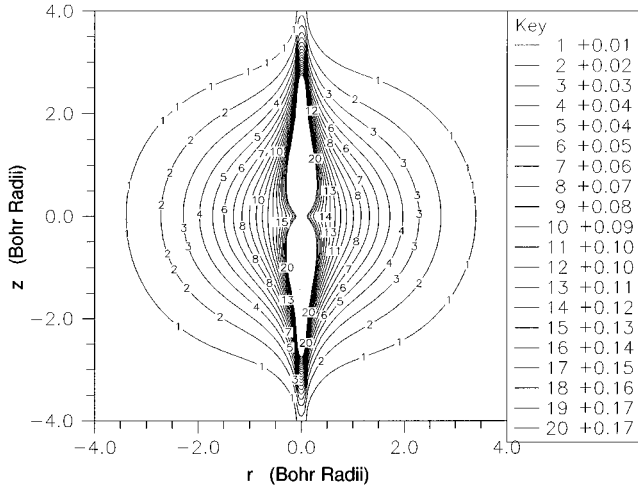


FIG. 12. Contour plot of  $\rho(x,z)$  for the quadratic Zeeman ground-state configuration based on Eq. (43) for  $B=0.1$ .

### C. Hydrogen molecular ion

Our final two-dimensional example is the hydrogen molecular ion  $H_2^+$ . Expressed in elliptic coordinates, the ( $l=0$ ) Hamiltonian becomes

$$\left[ \frac{\partial}{\partial \xi} (\xi^2 - 1) \frac{\partial}{\partial \xi} + \frac{\partial}{\partial \eta} (1 - \eta^2) \frac{\partial}{\partial \eta} \right] \Psi(\xi, \eta) + r_{AB}^2 \left[ \frac{1}{4} E' (\xi^2 - \eta^2) + \frac{e^2}{r_{AB}} \xi \right] \Psi(\eta, \xi) = 0, \quad (44)$$

where

$$\xi = \frac{r_A + r_B}{r_{AB}}, \quad \eta = \frac{r_A - r_B}{r_{AB}}, \quad E' = E - \frac{e^2}{r_{AB}}. \quad (45)$$

Expanding this wave function as

$$\Psi(\eta, \xi) = \sum_{i,j} a_{i,j} \xi^i \eta^j \exp\left(-\sqrt{\frac{r_{AB}^2 E'}{4}} \xi\right) \quad (46)$$

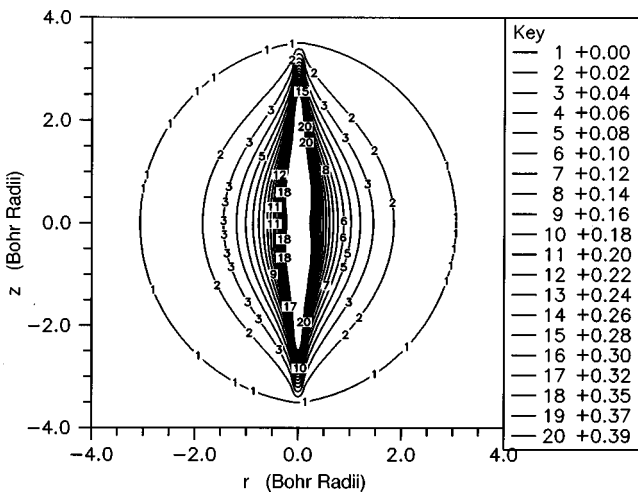


FIG. 13. Contour plot of  $\rho(x,z)$  for the quadratic Zeeman ground-state configuration based on Eq. (43) for  $B=2$ .

TABLE XI. First two symmetric energy levels for the hydrogen dimer ion  $H_2^+$  for selected separation distances  $r_{AB}$ .

$r_{AB}$	$E_{\text{ground}}$	$E_{\text{first excited}}$
1.0	-1.451 786 313 377	-0.422 924 588
1.5	-1.248 989 872 121 6	-0.388 600 912 1
2.0	-1.102 634 214 494 94	-0.360 864 875 33

allows us to generate a recursion relation that we used to obtain the ground- and first symmetric excited-state energies in Table XI for selected separation distances  $r_{AB} = |r_A - r_B|$ . In Fig. 14 we plot the ground-state energy versus the separation distance of the nuclei  $r_{AB}$ .

## V. SUMMARY

We have developed a multidimensional, iterative quantization procedure based on wave-function representations of the form  $\Psi = (\sum_i a_i [E, \dots] \xi^i) R(\xi)$ , involving some suitable reference function  $R$ . Upon identifying the convergent zeros, in the energy domain, of the power-series coefficients,  $a_i [E_n] = 0$ , highly accurate estimates for the  $n$ th state energy  $E_n$  and wave function  $\Psi_n$  were obtained. Our procedure is very algebraic in nature (although also implementable numerically) and lends itself well to algebraic software programming. We applied it to various prototypical problems in configuration ( $\xi=x$ ) and momentum ( $\xi=k$ ) space with great success.

## ACKNOWLEDGMENTS

We would like to thank J.-P. Antoine, C. M. Bender, D. Bessis, S. Böttcher, J. Cizek, S. T. Manson, R. Murenzi, A. Z. Msezane, R. G. Parr, A. Starace, and E. J. Weniger for fruitful discussions. This work was supported in part by the National Science Foundation under Grant No. HRD9450386, Air Force Office of Scientific Research under Grant No. F49620-96-1-0211, and Army Research Office under Grant No. DAAH04-95-1-0651.

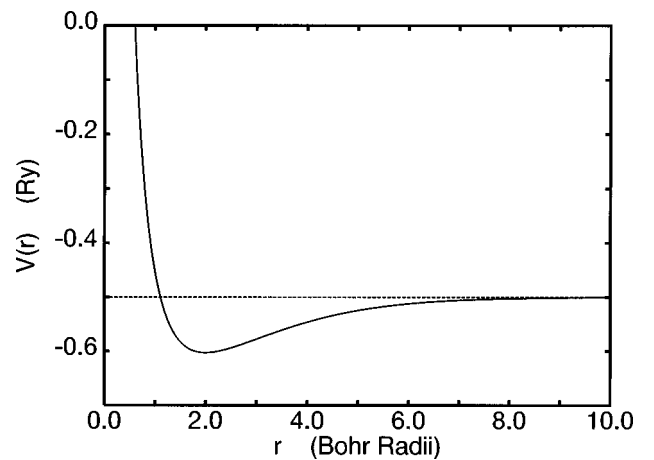


FIG. 14. Ground-state energy of  $H_2^+$  as a function of the interatomic distance  $r$ .

## APPENDIX

We present two arguments for the validity of Eq. (2). The first is more rigorous than the second, in that it requires one extra assumption. In each case, our objective is to understand how the power-series-generated coefficients of the wavefunction expansion  $\Psi(x) = (\sum_j a_j[E] x^j) R(x)$  relate to the coefficients generated through a Hill-determinant-based analysis, utilizing the nonorthogonal, complete, basis  $\mathcal{B}_i(x) \equiv x^i R(x)$ :  $\Psi(x) = \sum_i v_i[E] \mathcal{B}_i(x)$ .

For the Schrödinger-Hamiltonian eigenenergy problem  $H\Psi = E\Psi$ , let us take  $\Psi(x) = \sum_j v_j \mathcal{B}_j(x)$  and project unto the  $\mathcal{B}_i$  state through the equation  $\langle \mathcal{B}_i | H - E | \Psi \rangle = 0$ . Alternatively,  $\sum_j \mathcal{M}_{i,j}[E] v_j[E] = 0$ , where  $\mathcal{M}_{i,j}[E] = \langle \mathcal{B}_i | H | \mathcal{B}_j \rangle - E \langle \mathcal{B}_i | \mathcal{B}_j \rangle$ . The solution to this infinite set of matrix equations are the energy and  $v$  coefficients for the  $l$ th state:  $E_l^{(\text{exact})} \equiv E_l^{(\infty)}$  and  $v_j[E_l^{(\infty)}]$ .

The standard Galerkin approximation involves the  $I$ th-order truncation

$$\Psi^{(I)}(x) = \sum_{i=0}^I v_i \mathcal{B}_i(x), \quad (\text{A1})$$

leading to the  $I$ th-order equation

$$\sum_{j=0}^I \mathcal{M}_{i,j}[E_l^{(I)}] v_j[E_l^{(I)}] = 0, \quad (\text{A2})$$

involving the Hill-determinant equation

$$\text{Det}(\mathcal{M}^{(I)}[E_l^{(I)}]) = 0, \quad (\text{A3})$$

where  $\mathcal{M}_{ij}^{(I)} \equiv \mathcal{M}_{ij}$  for  $0 \leq i, j \leq I$ .

For a suitable basis the roots of the Hill determinant converge to the true eigenvalues of the Hamiltonian as  $I \rightarrow \infty$  ( $l$  indexes the roots):

$$\lim_{I \rightarrow \infty} E_l^{(I)} = E_l^{(\infty)}. \quad (\text{A4})$$

This is our assumption.

We now adopt a different notation for the  $v$  coefficients in order to emphasize the particular normalization prescription to be used:

$$\tilde{v}[E_l^{(I)}] \equiv \tilde{V}^{(I)}[E_l^{(I)}], \quad (\text{A5})$$

$$\sum_{j=0}^I \mathcal{M}_{i,j}[E_l^{(I)}] \tilde{V}_j^{(I)}[E_l^{(I)}] = 0$$

for  $0 \leq i \leq I$  where we normalize by  $V_l^{(I)} = 1$ . For sufficiently large values of the expansion order  $I$  we should have

$$V_j^{(I)}[E_l^{(I)}] \rightarrow \frac{a_j[E_l^{(I)}]}{a_l[E_l^{(I)}]} \quad (\text{A6})$$

for  $0 \leq j \leq I$  since each sequence of coefficients generates the same wave function

$$\sum_{j=0}^I V_j^{(I)}[E_l^{(I)}] x^j R_\beta(x) \rightarrow \sum_{j=0}^I \frac{a_j[E_l^{(I)}]}{a_l[E_l^{(I)}]} x^j R_\beta(x) \rightarrow \Psi_l(x). \quad (\text{A7})$$

In this context we equate the coefficients ( $a_l[E_l^{(I)}] \neq 0$ )

$$V_j^{(I)}[E_l^{(I)}] = \frac{a_j[E_l^{(I)}]}{a_l[E_l^{(I)}]} \quad (\text{A8})$$

for  $0 \leq j \leq I$ . Note that we are not necessarily extending this equality to the entire energy domain.

We now present our first proof of Eq. (2), based upon the preceding assumptions. There are two cases to be considered. The first corresponds to the simplest energy dependence for the  $a$  coefficients. The second generalizes things to include the dependence on the missing moment (or other similar) variables.

## 1. Proof 1

*Case 1:  $a_j[E]$  a rational fraction.* This corresponds to most one-dimensional configuration-space problems and some special momentum-space problems. The expression

$$\mathcal{P}_i[E] \equiv \sum_{j=0}^I \mathcal{M}_{i,j}[E] a_j[E] \quad (\text{A9})$$

will also be a rational fraction in  $E$  and continuous at  $E = E_l^{(I)}$ . From Eqs. (A8) and (A5) we have  $\mathcal{P}_i[E_l^{(I)}] = 0$ , as long as  $i \leq I$ . We are interested in evaluating

$$\mathcal{P}_{i \leq I-1}[E \rightarrow E_l^{(I-1)}]. \quad (\text{A10})$$

In this regard, the partial sum

$$\begin{aligned} & \sum_{j=0}^{I-1} \mathcal{M}_{i,j}[E_l^{(I-1)}] a_j[E_l^{(I-1)}] \\ &= a_{I-1}[E_l^{(I-1)}] \sum_{j=0}^{I-1} \mathcal{M}_{i,j}[E_l^{(I-1)}] V_j^{(I-1)}[E_l^{(I-1)}] \end{aligned} \quad (\text{A11})$$

is zero since the latter summation corresponds to Eq. (A5) for  $I \rightarrow I-1$ . Accordingly,

$$\mathcal{M}_{i,I}[E_l^{(I-1)}] a_I[E_l^{(I-1)}] = \mathcal{P}_i[E_l^{(I-1)}] \quad (\text{A12})$$

for  $0 \leq i \leq I-1$ .

Since  $\lim_{I \rightarrow \infty} (E_l^{(I-1)} - E_l^{(I)}) \rightarrow 0$  and

$$\mathcal{P}_i[E_l^{(I)}] = 0, \quad (\text{A13})$$

we then have (if  $\mathcal{M}_{i \leq I-1, I}[E_l^{(I-1)}] \neq 0$ )

$$\lim_{I \rightarrow \infty} a_I[E_l^{(I-1)}] = 0. \quad (\text{A14})$$

Therefore, the zeros of  $a_I[E]$  should converge to the physical energies.

*Case 2.* The more general case corresponds to

$$a_j[E, \vec{\chi}] = \sum_{\ell=0}^{m_s} D_{j,\ell}[E] \chi_\ell, \quad (\text{A15})$$

where the  $D_{j,\ell}[E]$ 's are rational fractions in  $E$ . The preceding proof applies provided one works with the continuous function  $\mathcal{P}_i[E, \vec{\chi}]$ , where  $\vec{\chi}$  is a unknown vector determined by the boundary conditions and  $\mathcal{P}_i[E, \vec{\chi}]$  satisfies  $\mathcal{P}_i[E_i^{(l)}, \vec{\chi}_i^{(l)}] = 0$ .

## 2. Proof 2

Our second proof will assume that Eq. (A8) extends to the energy domain, beyond the energy values explicitly noted (i.e., the  $E_i^{(l)}$ 's). More specifically, consider the expansions

$$\Psi_i^{(l+1)}(x) = \sum_{i=0}^{I+1} V_i^{(l+1)}[E_i^{(l+1)}] x^i R_\beta(x) \quad (\text{A16})$$

and [from Eq. (A8)]

$$\Psi_i^{(l+1)}(x) = \sum_{i=0}^{I+1} \frac{a_i[E_i^{(l+1)}]}{a_{I+1}[E_i^{(l+1)}]} x^i R_\beta(x). \quad (\text{A17})$$

If we assume that

$$V_i^{(l+1)}[E] = \frac{a_i[E]}{a_{I+1}[E]} \quad (\text{A18})$$

for  $0 \leq i \leq I+1$  and  $E \in [E_i^{(l)}, E_i^{(l+1)}]$ , then we can show that

$$a_{I+1}[E_i^{(l)}] = 0. \quad (\text{A19})$$

This follows from immediate properties of the  $V$  elements, as developed below.

Let  $E$  assume any value  $E = E_c$  for which the infinite matrix  $\mathcal{M}_{ij}[E_c]$  has no minor submatrix with zero determinant.

One can recursively generate, through an effective LU decomposition method, an infinite set of vectors  $\{\vec{V}^{(l)}[E_c] | 0 \leq l < \infty\}$  satisfying

$$\sum_{j=0}^I \mathcal{M}_{i,j}[E_c] V_j^{(l)} = 0 \quad (\text{A20})$$

for  $0 \leq i \leq I-1$  and

$$\sum_{j=0}^I \mathcal{M}_{I,j}[E_c] V_j^{(l)} = \mathcal{D}_I[E_c], \quad (\text{A21})$$

where  $V_i^{(l)} = 1$  and  $V_j^{(l)} = 0$  for  $j \geq I+1$ . One also has  $\text{Det}(\mathcal{M}^{(l)}[E_c]) = \prod_{i=0}^I \mathcal{D}_i[E_c]$ .

The relation in Eq. (A20) involves  $I$  constraints for  $I$  unknowns [recall  $V_i^{(l)} = 1$ , thus Eq. (A20) is actually an inhomogeneous relation]. The second relation, Eq. (A21), serves to define  $\mathcal{D}_I[E_c]$ .

For a given order  $I$ , the roots of Eq. (A21) corresponds to the roots of Eq. (A3)  $E = E_i^{(l)}$ , defined by (implicitly)  $\text{Det}(\mathcal{M}^{(l)}[E_i^{(l)}]) \neq 0$  and  $\text{Det}(\mathcal{M}^{(l)}[E_i^{(l)}]) = 0$ , or  $\mathcal{D}_I[E_i^{(l)}] = 0$ . We denote the corresponding vectors by  $V^{(l)}[E_i^{(l)}]$ .

From the recursion formulas for the  $V$ 's we have

$$V_i^{(l+1)}[E] = - \frac{\sum_{i=0}^I V_i^{(l)}[E] \mathcal{M}_{i,I+1}[E]}{\mathcal{D}_I[E]}. \quad (\text{A22})$$

Thus, in the  $E \rightarrow E_i^{(l)}$  limit, for a given  $l$ , one obtains

$$V_i^{(l+1)}[E_i^{(l)}] = \pm \infty, \quad (\text{A23})$$

provided the numerator expression in Eq. (68) does not simultaneously go to zero. The above infinite relation yields the desired result in Eq. (A19).

[1] C. M. Bender and S. A. Orszag, *Advanced Mathematical Methods for Scientists and Engineers* (McGraw-Hill, New York, 1978).  
 [2] C. J. Tymczak, G. S. Japaridze, C. R. Handy, and X.-Q. Wang, Phys. Rev. Lett. **80**, 3673 (1998).  
 [3] C. R. Handy, J. Maweu, and L. S. Atterbery, J. Math. Phys. **37**, 1182 (1996); C. R. Handy, Phys. Rev. A **46**, 1663 (1992).  
 [4] F. Vinette and J. Cizek, J. Math. Phys. **32**, 3392 (1986).  
 [5] W. Janke and H. Kleinert, Phys. Rev. Lett. **75**, 2787 (1995).  
 [6] F. Arias de Saavedra and E. Buendia, Phys. Rev. A **42**, 5073 (1990).  
 [7] (a) C. R. Handy and D. Bessis, Phys. Rev. Lett. **55**, 931

(1985); (b) C. R. Handy, D. Bessis, G. Sigismondi, and T. D. Morley, *ibid.* **60**, 253 (1988).  
 [8] C. R. Handy and R. Murenzi, Phys. Rev. A **54**, 3754 (1996); J. Phys. A **30**, 4709 (1997), and unpublished.  
 [9] C. R. Handy J. Phys. A **29**, 4093 (1996).  
 [10] C. R. Handy, J. Phys. A **18**, 3593 (1985).  
 [11] R. J. W. Hodgson, J. Phys. A **21**, 1563 (1988).  
 [12] C. R. Handy, H. Hayes, D. V. Stephens, J. Joshua, and S. Summerour, J. Phys. A **26**, 2635 (1993), refer to Eq. (2.5).  
 [13] E. R. Vrscaj and C. R. Handy, J. Phys. A **22**, 823 (1989).  
 [14] W. Rosner, G. Wunner, H. Herold, and H. Ruder, J. Phys. B **17**, 29 (1984).  
 [15] C. R. Liu and A. F. Starace, Phys. Rev. A **35**, 647 (1987).